Eur Biophys J (2005) 34: 285–293
DOI 10.1007/s00249-004-0450-z

ARTICLE

Andreas Hinz · Hans-Joachim Galla

Viral membrane penetration: lytic activity of a nodaviral fusion peptide

Received: 7 October 2004 / Revised: 19 November 2004 / Accepted: 22 November 2004 / Published online: 15 April 2005

Abstract The auto-cleavage product from the C-terminal part of the capsid protein of the flock house virus, namely the γ_1 peptide, was used as a model peptide to characterize the initial steps of viral membrane penetration. Monolayers at the air–water interface were used to investigate the phase behaviour of ternary lipid–peptide mixtures, whereas solid-supported membranes were used to visualize the lytic activity of the γ_1 peptide. 1,2-Dipalmitoyl-*sn*-glycero-phospatidylcholine/1,2-dipalmitoyl-*sn*-glycero-phospatidylserine (4:1) membranes were used as negatively charged model membranes. By means of film balance techniques lipid/peptide discrimination was found resulting in a lipid-rich and a peptide-rich phase. Quartz crystal microbalance and scanning force microscopy experiments led to the conclusion of a detergent-like mechanism of the γ_1 peptide resulting in mixed lipid–peptide micelles with a molar ratio of 2.8:1. A monolayer adsorption with an ongoing lysis of membranes was found with γ_1 peptide molecules interacting at membrane defects.

Keywords Quartz crystal microbalance · Scanning force microscopy · Solid-supported membranes · Flock house virus · Lipid/peptide discrimination · Fluorescence light microscopy

Abbreviations DPPC: 1,2-Dipalmitoyl-*sn*-glycero-phospatidylcholine · DPPS: 1,2-Dipalmitoyl-*sn*-glycero-phospatidylserine · EDTA: Ethylenediaminetetraacetic acid · HPLC: High-performance liquid chromatography · LUV: Large unilamellar vesicle · MLV: Multilamellar vesicle · OT: Octanethiol · QCM: Quartz crystal microbalance · SFM: Scanning force microscopy

A. Hinz · H.-J. Galla (✉)
Institut für Biochemie,
Westfälische Wilhelms-Universität Münster,
Wilhelm-Klemm-Strasse 2,
48149 Münster, Germany
E-mail: gallah@uni-muenster.de
Tel.: +49-251-8333200
Fax: +49-251-8333206

Introduction

Viral infections are initiated by peptide-mediated interactions between the host cell membrane and viral particles. Fusion peptides play the key role in entering cells by incorporation into the host cell membrane to facilitate viral genome transport. These peptides often supply a positive net charge to interact with negatively charged phospholipid membranes. For the treatment of viral infections it is of decisive relevance to understand these molecular mechanisms. In this study the fusion peptide of the flock house virus, namely the γ_1 peptide, was used as a model peptide to characterize viral peptide interactions with phospholipid model membranes.

The interactions of amphipathic positively charged peptides with phospholipid membranes have been intensively investigated and different molecular mechanisms have been introduced, but a clear understanding of these mechanisms has not been given yet (Shai 1999; Sitaram and Nagaraj 1999). The most accepted ones are the "carpet" mechanism (Pouny et al. 1992) and the "barrel-stave" mechanism (Ehrenstein and Lecar 1977). With the barrel-stave model the insertion of amphipathic α-helices into the hydrophobic core of phospholipid membranes to form transmembrane pores can be described. A further development of a model for peptide–membrane interactions concerning peptides with a high positive charge was given by the introduction of "toroidal pores" (Weakliem et al. 1995; Hallock et al. 2003). The pores or membrane channels are encased by a peptide envelope to enable the transport of charged molecules, e.g. RNA or DNA.

In contrast, peptides acting via the carpet mechanism are always in contact with the phospholipid headgroups and do not insert into the hydrophobic core of the membrane. Four steps of interactions are proposed. Binding of peptide molecules to the membrane is the

initial step of the carpet mechanism. It is followed by an alignment of peptide monomers to face the phospholipid headgroups with the hydrophilic surface of the peptides. After this step the peptide molecules rotate to reorientate their hydrophobic residues towards the hydrophobic core of the membrane. Finally a disintegration of the membrane appears by disrupting its curvature. An overview of peptide–lipid interactions via different mechanisms is given by Shai (1999).

The γ_1 peptide from the flock house virus was chosen as an example for the interactions of simple RNA viruses with 1,2-dipalmitoyl-*sn*-glycero-phospatidylserine (DPPC)/1,2-dipalmitoyl-*sn*-glycero-phospatidylserine (DPPS) (4:1) membranes as model membranes for negatively charged host cell membranes. The flock house virus is a small non-enveloped (+) single-stranded RNA virus from *Nodaviridae* that infects insects (Scotti et al. 1983). Viral particles consist of a single-stranded RNA genome with two different parts and only one coat protein in icosahedral asymmetric $T=3$ units (Dong et al. 1998). During infection the precursor protein α (44 kDa) of this coat protein undergoes a maturation cleavage at Asn363 to produce virion proteins β (363 amino acids) and γ (44 amino acids) (Kaesberg et al. 1990). The C-terminal part of the latter auto-cleavage product is an amphipathic α-helix, a so-called γ_1 peptide, containing 21 amino acids and a net positive charge of $z=+2$ (Fig. 1). For the γ_1 peptide used in this study a Met $\rightarrow$ Nle substitution at position 2 was used to prevent the synthetic γ_1 peptide from being oxidized (Bong et al. 2000).

Membrane binding and penetration by fusogenic peptides can be investigated using different biophysical techniques. Monolayer experiments at the air–water interface enable the determination of the binding activity of peptides (Pethica 1955; Brockman 1999; Maget-Dana 1999) as well as the characterization of the phase behaviour of phospholipid membranes (Lohner and Prenner 1999; Abuja et al. 2004). Recently, the quartz crystal microbalance (QCM) was introduced to determine binding constants of proteins to solid-supported phospholipid membranes (Janshoff et al. 2000). Scanning force microscopy (SFM) is used to visualize the topology of membranes or even cells (Radmacher et al. 1992; Engel et al. 1999; Janshoff and Steinem 2001). Using these biophysical techniques a more detailed view on the initial steps of nodaviral infection will be presented. Possible mechanisms are discussed and a classification of γ_1 peptide interactions with phospholipid membranes is given.

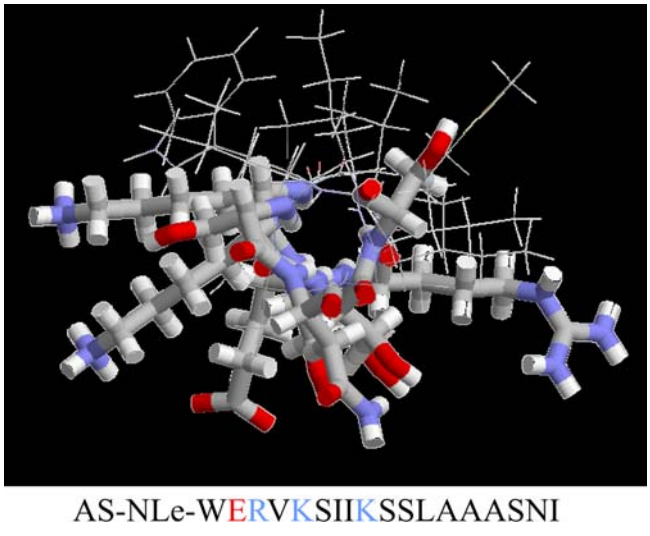

Fig. 1 Helical wheel diagram and amino acid sequence of the γ_1 peptide (*red* negative charge, *blue* positive charge). Polar and charged residues are shown as *balls* and *sticks*. A Met $\rightarrow$ Nle substitution was made to prevent the γ_1 peptide from being oxidized

Materials and methods

Materials

DPPC and DPPS were obtained from Avanti Polar Lipids (Alabaster, AL, USA) and were used without further purification. The γ_1 peptide was synthesized and purified by high-performance liquid chromatography (HPLC) by Affina (Berlin, Germany) with a purity of more than 96%. No modifications at the C-terminus and the N-terminus were used. Octanethiol (OT) was obtained from Sigma (Taufkirchen, Germany); chloroform and methanol were HPLC grade and were obtained from Merck (Darmstadt, Germany). All experiments were performed in phosphate buffer (10 mM NaH_2PO_4/Na_2HPO_4, 0.1 M NaCl, 0.1 mM ethylenediaminetetraacetic acid, EDTA, pH 7.4) at 20°C.

Preparation of monolayers

Phospholipids were dissolved in methanol/chloroform (1:1, v/v) to a final concentration of 0.5 mM. The γ_1 peptide was used as methanolic solution. Solutions were stored at −20°C for a maximum of 3 months. Monolayers were prepared by spreading the lipid solutions with a syringe obtained from Hamilton (Bonaduz, Switzerland) dropwise on the aqueous surface of the Langmuir film balance at a surface pressure of 0–0.1 mN m^{-1}. The lipid films were equilibrated for 15 min prior to compression.

Concentration of the γ_1 peptide

The concentration of the γ_1 peptide was measured by UV/vis absorption at a wavelength of 280 nm. The extinction coefficient was determined to be 5,570 l mol^{-1} cm^{-1} (Bong et al. 1999). Hinz (2003) showed that there is no significant change in the extinction coefficient in methanolic solution.

Film balance measurements

Isotherms of mixed γ_1 peptide/phospholipid monolayers at the air–water interface were measured on a Langmuir

film balance developed by Riegler & Kirstein (Mainz, Germany) with a Wilhelmy-plate system at 20°C. A phosphate buffer (10 mM NaH_2PO_4/Na_2HPO_4, 0.1 M NaCl, 0.1 mM EDTA, pH 7.4) was used as a subphase. Monolayers were compressed with a velocity of 2.9 cm^2 min^{-1}.

Preparation of solid-supported membranes for QCM measurements

QCM measurements were performed on gold-covered quartz-crystal-supported OT/phospholipid bilayers. Phospholipids were dissolved in methanol/chloroform (1:1, v/v), dried under a steam of nitrogen at 50°C, and the remaining solvents were evaporated for 2 h at 50°C. The lipid films were stored at 4°C. Multilamellar vesicles (MLVs) were prepared by redissolving the lipid films in phosphate buffer to a final concentration of 1 mg ml^{-1}. The emulsions were equilibrated at 50°C for 15 min and vortexed three times for 1 min. MLV solutions were pressed 21 times through a polycarbonate membrane in a Liposofast miniextruder from Avestin (Ottawa, Canada) to get large unilamellar vesicles (LUVs) with a diameter of 100 nm. Gold-covered quartz crystals were fixed in a Teflon chamber and incubated with 2 mM ethanolic OT solution for 30 min at room temperature. The remaining OT was rinsed five times with ethanol and afterwards with buffer solution. Freshly prepared LUV solution was diluted one time with buffer and the OT-functionalized quartz crystals were incubated for 1 h at 50°C. Finally supernatant LUVs were removed with buffer solution.

Langmuir–Blodgett transfer of monolayers for SFM investigations

SFM investigations were performed on mica-supported phospholipid bilayers. A DPPC monolayer was compressed on a Langmuir film balance, equilibrated at a surface pressure of 45 mN m^{-1} and afterwards transferred by the Langmuir–Blodgett technique to a mica sheet with a velocity of 0.7 mm min^{-1}. This layer sticks more strongly to mica sheets than mixed DPPC/DPPS ones (Janshoff et al. 2001). In a second step a DPPC/DPPS (4:1) monolayer was compressed and equilibrated at a surface pressure of 30 mN m^{-1} and the mica sheet was pushed through the monolayer into the subphase to get an asymmetric DPPC–DPPC/DPPS (4:1) membrane. The mica sheets were fixed in a Teflon chamber that was filled up with buffer solution.

Quartz crystal microbalance

Quartz resonators were functionalized with an OT/phospholipid bilayer as described previously. The resonance frequency of the quartz crystals was analysed with a TTL SN74LS124N oscillator unit from Texas Instruments (Dallas, TX, USA) and recorded with a 53181A frequency counter from Hewlett-Packard (San Diego, CA, USA). The quartz resonators were fixed in a Teflon chamber and kept at 20°C in a Faraday cage. A constant flow of 0.35 ml min^{-1} within the aqueous circuit was driven with a Reglo Digital model 333 peristaltic pump from Ismatec (Wertheim-Mondfeld, Germany).

Scanning force microscopy

SFM images were taken in tapping mode with a BioScope/NanoScope IIIA controller from Digital Instruments (Santa Barbara, CA, USA). V-shaped silicon nitride cantilevers (type DNP, Veeco Instruments, Santa Barbara, CA, USA) with a spring constant of 0.6 N m^{-1} were used.

Results

Lipid/peptide discrimination

Compression isotherms of γ_1 peptide monolayers were measured on a phosphate-buffered subphase (Fig. 2a). The amphipathic γ_1 peptide shows a collapse surface pressure at about 27 mN m^{-1}, leading to an irreversible loss of γ_1 peptide molecules to the subphase. By means of compression/expansion cycles the loss of γ_1 peptide molecules is observed as a shift of the isotherms to lower molecular areas (data not shown). This collapse surface pressure is indicated by a plateau within the isotherms, in the following named "peptide plateau". The molecular area of the γ_1 peptide at the air–water interface was determined to be 474 $Å^2$ (Fig. 2a). DPPC/DPPS (4:1) monolayers were doped with various amounts of the γ_1 peptide in a range between 0 and 10 mol% of the total phospholipid amount. Compression isotherms of these ternary mixtures are shown in Fig. 2b. The phase transition from the liquid expanded (l_e) to the liquid-crystalline (l_c) phase of the lipids appears as a co-existence region at a surface pressure of about 3–5 mN m^{-1}, in the following named "lipid plateau". With increasing amount of γ_1 peptide this lipid plateau is shifted to higher molecular areas owing to the fact that only the total lipid amount is taken into account in calculating the concentration of the surface film. The average surface pressure of this plateau increases slightly with a cumulative amount of γ_1 peptide. At a surface pressure of about 26 mN m^{-1} the peptide plateau is observable, and can be identified as the collapse surface pressure of the γ_1 peptide. This plateau indicates the partial immiscibility of the γ_1 peptide in DPPC/DPPS (4:1) monolayers in the l_c phase leading to a phase separation into a lipid-rich and a peptide-rich phase. The assumption of a phospholipid/γ_1 peptide discrimination

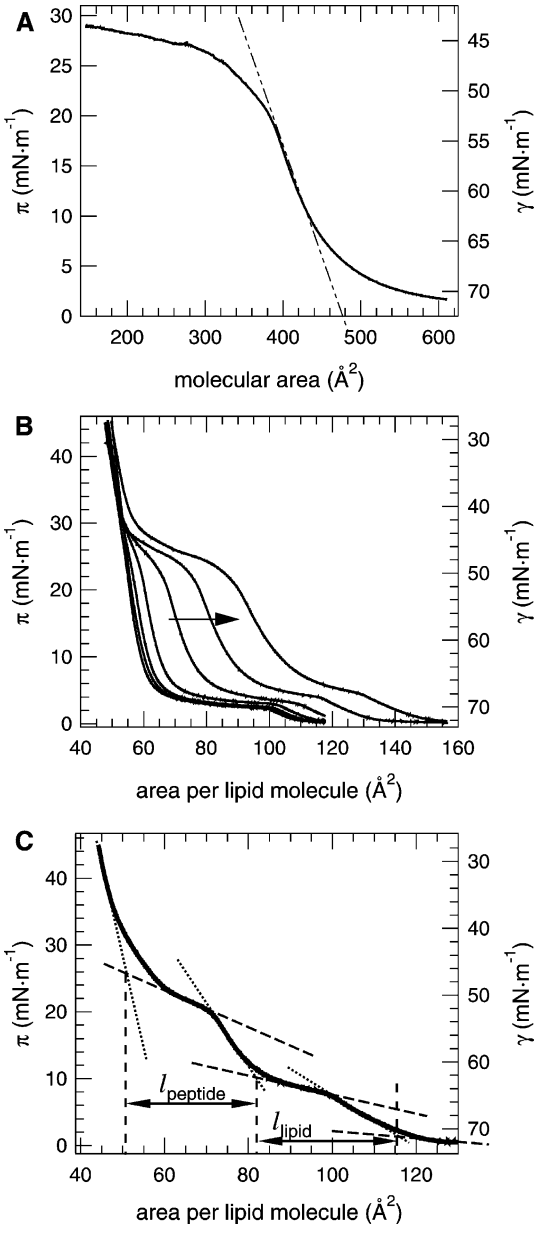

Fig. 2 **a** Compression isotherm of the γ_1 peptide. The *dashed line* indicates a molecular area of 474 Å^2. **b** Compression isotherms of 1,2-dipalmitoyl-*sn*-glycero-phospatidylcholine (*DPPC*)/1,2-dipalmitoyl-*sn*-glycero-phospatidylserine (*DPPS*) (4:1) monolayers with various amounts of the γ_1 peptide. The *arrow* indicates an increasing amount of γ_1 peptide: 0, 0.5, 1, 2, 4, 7 and 10% of the total lipid amount. **c** Determination of inflection points to characterize the length of the "lipid plateau" and the "peptide plateau" in compression isotherms

is consistent with the observation of a cumulative "plateau length" of the peptide plateau with increasing amount of the γ_1 peptide. This length is defined as the difference in molecular area between the onset and the offset of the plateaus that are indicated by inflection points of the isotherms (Fig. 2c). The degree of phase separation between a peptide-rich and a lipid-rich region is characterized by the plateau length of the

Table 1 Plateau lengths and average lateral pressures of the "lipid plateaus" and "peptide plateaus" of 1,2-dipalmitoyl-*sn*-glycero-phospatidylcholine/1,2-dipalmitoyl-*sn*-glycero-phospatidylserine (4:1) monolayers doped with various amounts of the γ_1 peptide. For definitions, see Fig. 2c and the text.

γ_1 peptide (mol%)	Lipid plateau		Peptide plateau	
	Plateau length (Å^2)	Plateau height (mN m^{-1})	Plateau length (Å^2)	Plateau height (mN m^{-1})
0	41.0	2.5	0	ND
0.5	39.0	3.0	2.0	28.5
1	37.5	3.0	4.0	27.0
2	35.0	3.5	6.0	27.0
4	32.0	4.0	12.5	26.0
7	28.0	5.0	22.0	26.0
10	24.0	5.5	29.5	25.5

plateaus within the isotherms (Table 1). A higher number of peptide-rich domains is observable as an increasing length of the peptide plateau. At high surface pressures above 40 mN m^{-1} the γ_1 peptide is totally squeezed out of the monolayers indicated by the identity of all isotherms in this surface pressure range. Compression/expansion cycles have shown that fractions of the γ_1 peptide can re-incorporate into the monolayer (data not shown).

Affinity of the γ_1 peptide for DPPC/DPPS (4:1) monolayers

In order to determine the binding constant of the γ_1 peptide and DPPC/DPPS (4:1) membranes, binary lipid monolayers were spread on the surface of a Langmuir film balance, and after equilibration at an initial surface pressure (π_0) various concentrations of the γ_1 peptide (c_γ) were injected into the subphase (Fig. 3a). The increase in surface pressure ($\Delta\pi$) was determined and plotted versus the concentration c of the γ_1 peptide in the subphase (Fig. 3b). A Gibbs–Langmuir adsorption isotherm (see the "Appendix") was used to fit the data following Eq. 1 and to calculate the binding constant (K_d):

$$\Delta\pi = \Gamma_{max} RT \ln\left(1 + K_d^{-1} c\right), \quad (1)$$

with Γ_{max} as the surface excess of the γ_1 peptide, R as the gas constant and T as the absolute temperature. A binding constant of 2.8 ± 1.2 nM was obtained.

As shown in Fig. 3a the surface pressure increases after γ_1 peptide injection. Above a critical γ_1 peptide concentration of about 20 nM a subsequent decrease in surface pressure occurs. This two-step reaction is a consequence of the initial adsorption of γ_1 peptide molecules to the monolayer and the following insertion into it. Hydrophobic interactions between phospholipid and γ_1 peptide molecules reduce the surface pressure. This effect has been described as well for the actin

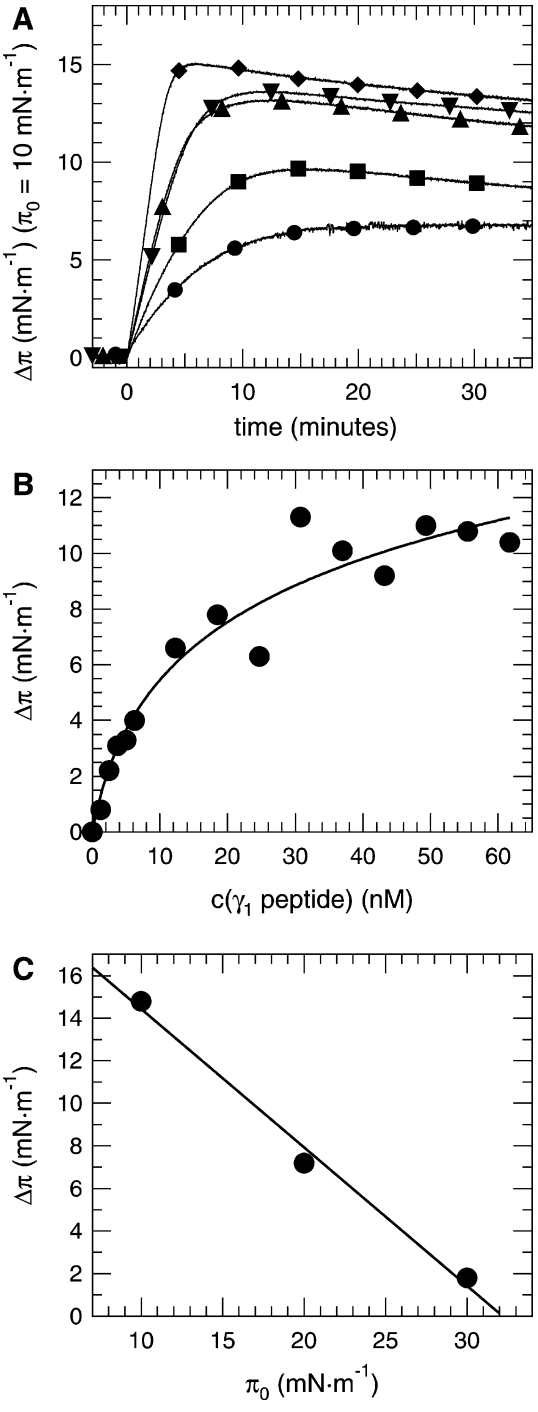

Fig. 3 **a** Increase of surface pressure ($\Delta\ \pi$) of DPPC/DPPS (4:1) monolayers as a function of time after injection of the γ_1 peptide into the phosphate-buffered subphase at an initial surface pressure of $\pi_0 = 10$ mN m^{-1}. The *symbols* indicate various γ_1 peptide concentrations: 12.3 nM (*circles*), 24.7 nM (*squares*), 37.0 nM (*up triangles*), 49.3 nM (*inverted triangles*) and 61.7 nM (*diamonds*). **b** Gibbs–Langmuir adsorption isotherm of the γ_1 peptide and DPPC/DPPS (4:1) monolayers. The *line* represents the result of a least-squares fit of the data following Eq. 1. The binding constant (K_d) was determined to be 2.8 ± 1.2 nM. **c** $\Delta\pi_{max}$ as a function of the initial surface pressure π_0. The *line* indicates a linear regression to calculate the critical initial surface pressure up to which the penetration of DPPC/DPPS (4:1) monolayers occurs

binding protein (Goldmann et al. 1999). In a second step a desorption from the monolayer surface is mediated through micellelike structures of phospholipid and γ_1 peptide molecules. Higher initial surface pressures lead to a smaller absolute increase in surface pressure after γ_1 peptide injection (Fig. 3c). Pethica (1995) introduced the critical surface pressure of monolayers up to which penetration is feasible. The integration of several peptides and proteins in phospholipid monolayers has been investigated and critical surface pressures between 25 and 32 mN m^{-1} have been reported (Sospedra et al. 1999; Trommeshauser et al. 1999). These data are in good agreement with the critical surface pressure of 32 mN m^{-1} for the γ_1 peptide and DPPC/DPPS (4:1) monolayers in our work.

Membrane disruption

QCM investigations on the lytic activity of the γ_1 peptide on solid-supported membranes

The desorption of phospholipids from the air–water interface into the subphase owing to interactions with the γ_1 peptide are the first hints to the carpet mechanism of the γ_1 peptide. Solid-supported membranes were furthermore used to characterize the kinetics of γ_1 peptide and phospholipid membrane interactions.

QCM measurements evidence the adsorption of γ_1 peptide molecules to solid-supported DPPC/DPPS (4:1) membranes as a decrease in resonance frequency of the quartz crystals of (3 ± 1) Hz (Fig. 4, trace a). This

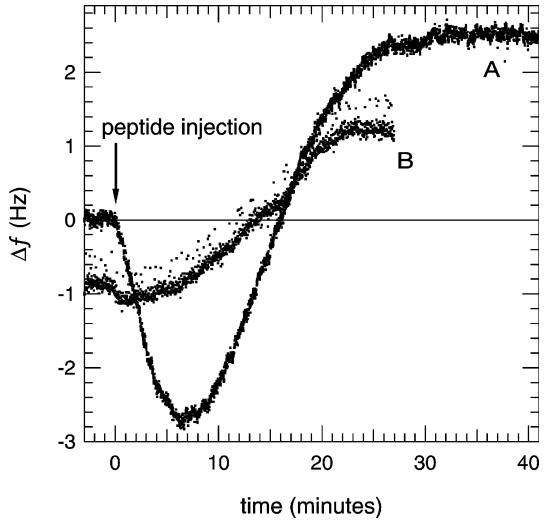

Fig. 4 Adsorption and lytic activity of the γ_1 peptide in a quartz crystal microbalance experiment. Octanethiol–DPPC/DPPS (4:1) was used as solid-supported membranes. The γ_1 peptide was injected at $t = 0$ min at a total concentration of 1.1 μM (*a*) and 0.12 μM (*b*). The decrease in resonance frequency corresponds to the adsorption of a γ_1 peptide monolayer (*a*), whereas the following increase of the resonance frequency is related to the desorption of one third of the phospholipid membrane in mixed phospholipid/γ_1 peptide micelles (*a*, *b*)

process takes about 5 min and is followed by the desorption of surface-bound material. Overall a total increase in resonance frequency of (2.6 ± 1) Hz is observed after more than half an hour (Fig. 4). This two-step reaction is similar to that observed by film-balance techniques.

Assuming the desorption of mixed γ_1 peptide/phospholipid micelles the total amount of desorbed material can be calculated. With an average molecular area of 43 Å^2 and an average molecular mass of 739 g mol^{-1} for DPPC/DPPS (4:1) membranes, and an electrode area of 0.265 cm^2, the total lipid amount on the quartz crystals can be calculated to be about 100 pmol. Using the integral mass sensitivity of 0.036 Hz cm^2 ng^{-1} for 5-MHz quartz crystals reported by Janshoff and coworkers (1996, 1997) an increase of 2.6 Hz is correlated to a lipid mass of 19.1 ng, which can be interpreted as the disruption of one quarter of the lipid membrane. The decrease in resonance frequency corresponds to a complete monolayer adsorption of the γ_1 peptide (9.3 pmol) assuming a molecular area of 474 Å^2 (Hinz 2003). Taking these calculations into account, one can assume that mixed γ_1 peptide/phospholipid micelles with a molar ratio of 1:2.8 are built, and desorb from the quartz crystal surface.

Topology of disrupted membranes visualized by means of SFM

The disturbance of membrane topology is visualized both as static and dynamic interactions with the γ_1 peptide. Static analysis of Langmuir–Blodgett transferred mixed DPPC/DPPS/γ_1 peptide (80:20:2) membranes on a mica support at a lateral pressure of 25 mN m^{-1} reveal circular and aggregated circular regions with a diameter of about 400 nm (Fig. 5). These domains appear as holes within the membrane with a depth of 3 nm, thus spanning the upper, water-exposed part of the membrane.

A dynamic analysis of γ_1 peptide and DPPC/DPPS (4:1) membranes is shown in Fig. 6. DPPC/DPPS (4:1) membranes were transferred to DPPC-coated mica and incubated with the γ_1 peptide. The time course of the membrane topology exhibits the interaction of the γ_1 peptide at membrane defects. Artificial pinholes (with a diameter of several nanometres) were already present in the membrane prior to γ_1 peptide exposure owing to the Langmuir–Blodgett transfer. During incubation these pinholes grow in size and after 3 h the area of the holes increased by a factor of 500%. No increase of the size of small pinholes within the membranes was observed in control experiments without any γ_1 peptide. The adsorption of γ_1 peptide molecules was a diffusion-controlled reaction owing to the lack of a continuous mixed solution. Therefore, the time scale is much longer than in the QCM experiments. A height and size analysis is given in Fig. 6g. All membrane holes that appear after 3 h were present prior to γ_1 peptide incubation at least as membrane defects.

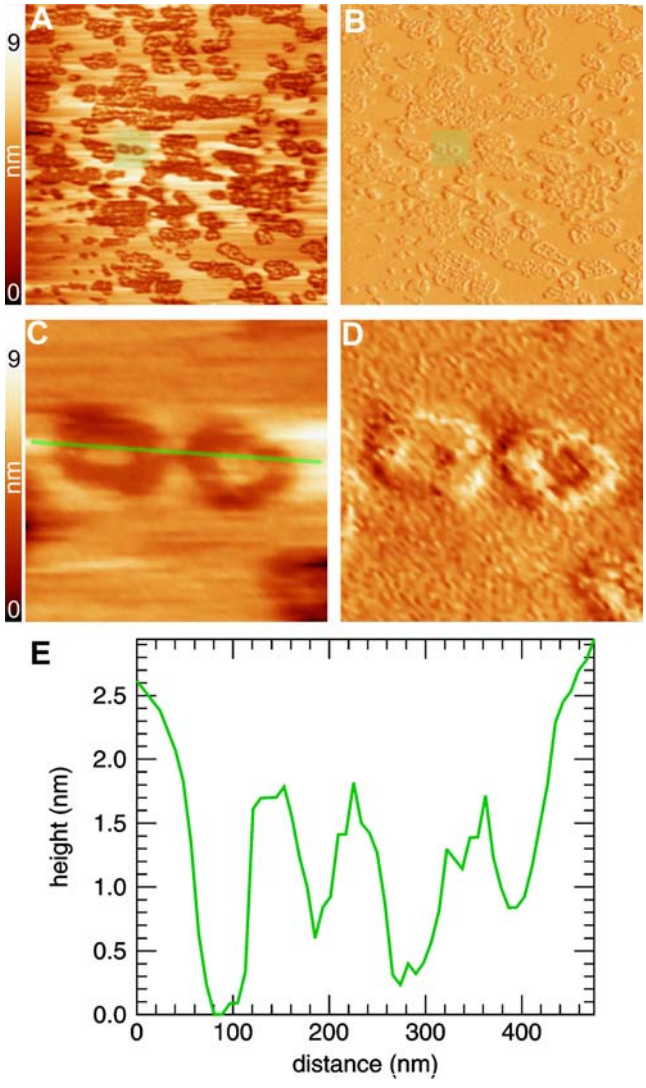

Fig. 5 Scanning force microscopy (*SFM*) images of a DPPC–DPPC/DPPS/γ_1 peptide (80:20:2) bilayer on mica at a lateral pressure of 25 mN m^{-1}. Image size 4.1×4.1 μm^2. The images were taken in contact mode and show the result of a height (**a**) and a deflection analysis (**b**). The *green shadowed areas* are enlarged in **c** and **d**. **e** Height analysis along the green line in **c**

Discussion

Lipid/peptide discrimination

The molecular area of the γ_1 peptide (474 Å^2) fits well with the molecular area of other amphipathic α-helical peptides such as bombolittin III (480 Å^2, 17 amino acids, Peggion et al. 1997), or maculatin 1.1 (280 Å^2, 21 amino acids, Ambroggio et al. 2004). The α-helical character of the γ_1 peptide when interacting with phospholipid membranes was proven by Janshoff et al. (1999) with circular dichroism studies.

Monolayer experiments at the air–water interface reveal the partial immiscibilty of the γ_1 peptide and DPPC/DPPS (4:1) membranes. Saturated lipids were

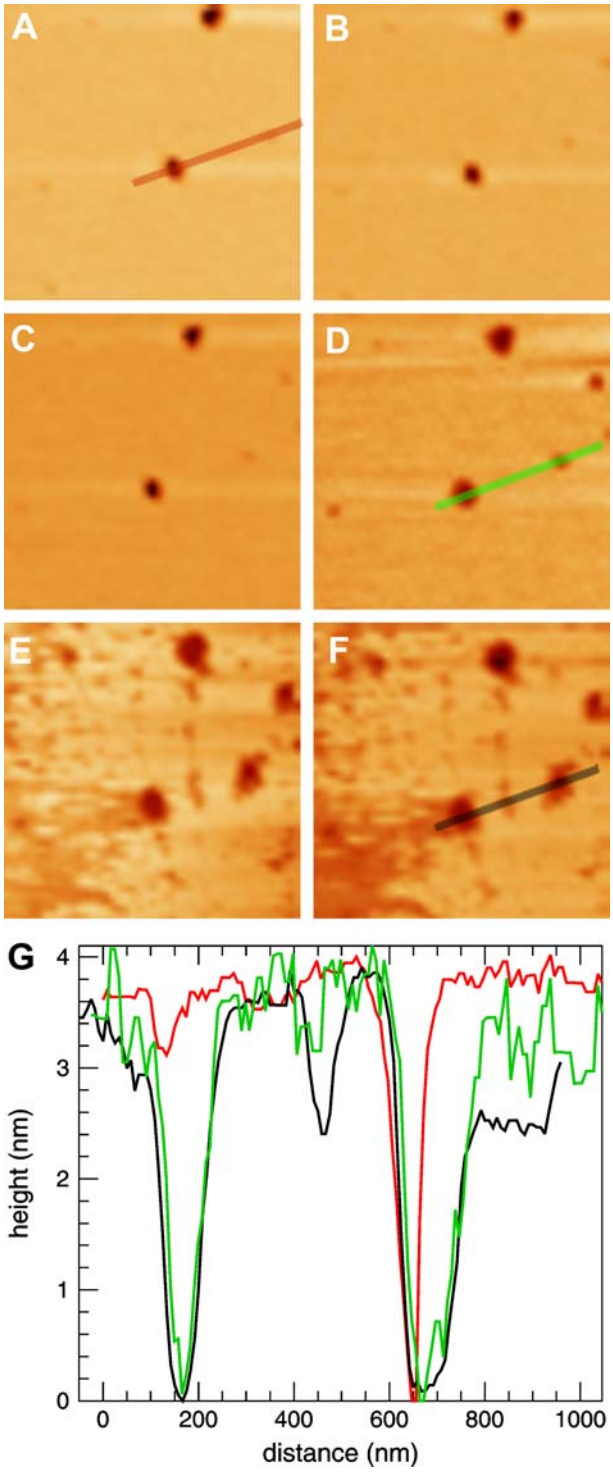

Fig. 6 Dynamic analysis of membrane disruption by means of SFM. Images were taken before (**a**) and 30 min (**b**), 60 min (**c**), 90 min (**d**), 150 min (**e**) and 180 min (**f**) after γ_1 peptide injection ($c = 1$ μM). No increase of the size of small pinholes within the membranes were observed in control experiments without any γ_1 peptide (images not shown). The height analysis of the *coloured lines* in **a**, **d** and **f** is given in **g**

chosen to avoid additional influences by double bonds and to minimize temperature effects on the acyl chains. The collapse surface pressure of the γ_1 peptide as well as the phase transition of the DPPC/DPPS (4:1) monolayers from the liquid expanded (l_e) to the liquid-crystalline (l_c) phase indicate a phase separation in a lipid-rich and a peptide-rich phase. These observations have already been reported for other viral or anti-microbial peptides (Ma et al. 1998; Konovalov et al. 2002; Trommeshauser and Galla 1998). A general miscibility in lipid regions with a negative charge and an immiscibility in DPPC-rich domains was found. Lipid discrimination induced by anti-microbial peptides has been reviewed by Lohner and Prenner (1999).

Van Mau et al. (1999) and Vié et al. (2000) reported a phase separation in mixed positively charged vector peptide/dioleoylphosphatidylcholine membranes as a consequence of hydrophobic peptide–peptide interactions. In the case of WALP peptides the incorporation of peptide molecules into phospholipid bilayers led to the formation of striated domains of high order (Rinia and coworkers 2000, 2002). The authors propose a model in which peptide molecules have a mismatch with surrounding lipid molecules, leading to a contraction of the membrane at the boundary between lipid and peptide molecules. The formation of peptide-rich domains within the monolayer is similar to the function of viral particles that also discriminate lipid-rich and peptide-rich phases on the surface of host cells. The capsid protein as the initial active agent of the virus is localized to a high degree (e.g. flock house virus with 180 meres of the γ_1 peptide) on the surface of the viral particle and is therefore enriched when interacting with the target membrane. There is also the necessity of aggregation of peptide molecules at the membrane surface to act either as pore-forming or membrane-lytic agents. Pore formation of amphipathic peptides is related to an encasement of the pore with peptide molecules to face both the hydrophobic core of the membrane as well as the hydrophilic water-filled channel. Lysis of parts of the membrane via mixed micelles is also related to an aggregation of peptide molecules at the membrane surface to achieve the necessary concentration to form these micelles. As a conclusion the lipid/peptide discrimination induced by the γ_1 peptide is a requirement for viral activity of the flock house virus.

Membrane disruption

Dynamic investigations of the interactions between the γ_1 peptide and phospholipid membranes indicate a two-step reaction. The initial binding of γ_1 peptide molecules was measured both as an increase in surface pressure within monolayers as well as a decrease in resonance frequency within solid-supported membranes. By means of the QCM a complete monolayer of γ_1 peptide molecules on the phospholipid membrane was observed. As a following step a re-arrangement within the membrane occurs, and this is followed by the desorption of membrane material. Calculations made from the results of QCM investigations reveal a membrane disruption and

the formation of mixed γ_1 peptide/lipid micelles with a molar ratio of 1:2.8. NMR studies on the formation of isotropic NMR peaks formed by the action of equinatoxin II on lipid membranes support the formation of micelles (Bonev et al. 2003). At this point a detergent-like mechanism such as the carpet mechanism can be assumed to describe the interactions of the γ_1 peptide and phospholipid membranes best.

Images taken with the scanning force microscope show pores with diameters in the range of viral particles (50–500 nm). The appearance of peptide-induced membrane pores was also reported by You et al. (2003), who found circular pores with a diameter of 200 nm when saposin C interacts with phospholipid membranes, and by Zhang et al. (2002), who reported the integration of protegrin-1 into phospholipid membranes by the formation of holes that span only the buffer-exposed part of the membrane. These observations correspond to the static analysis of mixed γ_1 peptide/phospholipid membranes which contain circular pores spanning the upper side of the membrane. Interactions of virions with cells were visualized by Kuznetsov et al. (2002), who were able to depict viral-induced pores in fibroblasts with a diameter of 200 nm. These results demonstrate a general scheme of peptide enrichment within phospholipid membranes to enable viral genome transport.

The second step of material desorption from the membrane surface was visualized as an increase in the size of artificial pores within the membrane. These membrane defects support the binding and lytic activity of the γ_1 peptide. The loss of membrane material was characterized to be one third of the solid-supported membrane, which results in mixed γ_1 peptide/phospholipid micelles with a molar ratio of 1:2.8. Desorption of membrane material was demonstrated by Ha et al. (2000), who investigated indolicidin. This peptide binds to the membrane surface, forms mixed lipid/peptide micelles that desorb from the surface, and afterwards peptide molecules fill the original holes inside the membrane.

As a conclusion, the carpet mechanism seems to be favoured by the γ_1 peptide. Its lytic activity leads to the formation of mixed γ_1 peptide/phospholipid micelles. The partial lysis of the target membrane and the formation of pores on the same order of magnitude as virions enable viral genome transport into the host cell.

Acknowledgements The authors would like to thank Sebastian Schrot for fruitful discussion and technical support in the SFM investigations, and Daniel Breitenstein for a critical review of the manuscript. This work was supported by the Deutsche Forschungsgesellschaft under grant Sonderforschungsbereich 424

Appendix

The Gibbs–Langmuir adsorption isotherm is derived from the Gibbs isotherm

$$\Gamma = -\frac{c}{RT}\frac{\partial\gamma}{\partial c}, \tag{2}$$

with the surface tension γ, the bulk concentration of the γ_1 peptide, the gas constant R, the absolute temperature T, and the Langmuir isotherm

$$\Gamma = \Gamma_{\max}\frac{K_{\mathrm{d}}^{-1}c}{1+K_{\mathrm{d}}^{-1}c}, \tag{3}$$

with the binding constant K_{d}^{-1} and the surface excess of the γ_1 peptide. The integration

$$\int_{\gamma_0}^{\gamma(c)} \partial\gamma = -\Gamma_{\max}RT\int_0^c \frac{K_{\mathrm{d}}^{-1}}{1+K_{\mathrm{d}}^{-1}c}\partial c \tag{4}$$

leads to the final form, which was used to fit the data in Fig. 3b:

$$\gamma(c) = \gamma_0 - \Gamma_{\max}RT\,\ln\left(1+K_{\mathrm{d}}^{-1}c\right). \tag{5}$$

References

Abuja PM, Zenz A, Trabi M, Craik DJ, Lohner K (2004) The cyclic antimicrobial peptide RTD-1 induces stabilized lipid–peptide domains more efficiently than its open-chain analogue. FEBS Lett 566:301–306

Ambroggio EE, Separovic F, Bowie J, Fidelio GD (2004) Surface behaviour and peptide–lipid interactions of the antibiotic peptides Maculatin and Citropin. Biochim Biophys Acta 1664:31–37

Bonev BB, Lam YH, Anderluh G, Watts A, Norton RS, Separovic F (2003) Effects of the eucaryotic pore-forming cytolysin Equinatoxin II on lipid membranes and the role of sphingomyelin. Biophys J 84:2382–2392

Bong DT, Steinem C, Janshoff A, Johnson JE, Ghadiri MR (1999) A highly membrane-active peptide in flock house virus: implications for the mechanism of nodavirus infection. Chem Biol 6:473–481

Bong DT, Janshoff A, Steinem C, Ghadiri MR (2000) Membrane partitioning of the cleavage peptide in flock house virus. Biophys J 78:839–845

Brockman H (1999) Lipid monolayers: why use half a membrane to characterize protein–membrane interactions? Curr Opin Struct Biol 9:438–443

Dong XF, Natarajan P, Tihova M, Johnson JE, Schneemann A (1998) Particle polymorphism caused by deletion of a peptide molecular switch in a quasiequivalent icosahedral virus. J Virol 72:6024–6033

Ehrenstein G, Lecar H (1977) Electrically gated ionic channels in lipid bilayers. Q Rev Biophys 10:1–34

Engel A, Gaub HE, Müller DJ (1999) Atomic force microscopy: a forceful way with single molecules. Curr Biol 9:R133–R136

Goldmann WH, Theodoridis JM, Sharma CP, Hu B, Isenberg G (1999) Fragments from actin binding protein (ABP-280; filamin) insert into reconstituted lipid layers. Biochem Biophys Res Commun 259:108–112

Ha TH, Kim CH, Park JS, Kim K (2000) Interaction of indolicidin with model lipid bilayer: quartz crystal microbalance and atomic force microscopy study. Langmuir 16:871–875

Hallock KJ, Lee DK, Ramamoorthy A (2003) MSI-78, an analogue of the magainin antimicrobial peptides, disrupts lipid bilayer structure via positive curvature strain. Biophys J 84:3052–3060

Hinz A (2003) Insights into viral membrane penetration: biophysical investigations on the fusogenic peptide of the Flock House Virus with phospholipid model membranes. Schueling, Muenster

Janshoff A, Steinem C (2001) Scanning force microscopy of artificial membranes. ChemBioChem 2:798–808

Janshoff A, Steinem C, Sieber M, Galla HJ (1996) Specific binding of peanut agglutinin to G_{M1}-doped solid supported lipid bilayers investigated by shear wave resonator measurements. Eur Biophys J 25:105–113

Janshoff A, Steinem C, Sieber M, el Bayâ A, Schmidt MA, Galla HJ (1997) Quartz crystal microbalance investigation of the interaction of bacterial toxins with ganglioside containing solid supported membranes. Eur Biophys J 26:261–270

Janshoff A, Bong DT, Steinem C, Johnson JE, Ghadiri MR (1999) An animal virus-derived peptide switches membrane morphology: possible relevance to nodaviral transfection processes. Biochemistry 38:5328–5336

Janshoff A, Galla HJ, Steinem C (2000) Piezoelectric mass-sensing devices as biosensors—an alternative to optical biosensors? Angew Chem Int Ed 39:4004–4032

Janshoff A, Ross M, Gerke V, Steinem C (2001) Visualization of Annexin I binding to Calcium-induced phosphatidylserine domains. ChemBioChem 7(8):587–590

Kaesberg P, Dasgupta R, Sgro JY, Wery JP, Selling BH, Hosur MV, Johnson JE (1990) Structural homology amoung four nodaviruses as deduced by sequencing and X-ray crystallography. J Mol Biol 214:423–435

Konovalov O, Myagkov I, Struth B, Lohner K (2002) Lipid discrimination in phospholipid monolayers by the antimicrobial frog skin peptide PGLa. A synchrotron X-ray grazing incidence and reflectivity study. Eur Biophys J 31:428–437

Kuznetsov YG, Datta S, Kothari NH, Greenwood A, Fan H, McPherson A (2002) Atomic force microscopy investigation of fibroblasts infected with wild-type and mutant murine leukemia virus (MuLV). Biophys J 83:3665–3674

Lohner K, Prenner EJ (1999) Differential scanning calorimetry and X-ray diffraction studies of the specificity of the interaction of antimicrobial peptides with membrane-mimetic systems. Biochim Biophys Acta 1462:141–156

Ma J, Koppenol S, Yu H, Zografi G (1998) Effects of a cationic and hydrophobic peptide, KL4, on model lung surfactant lipid monolayers. Biophys J 74:1899–1907

Maget-Dana R (1999) The monolayer technique: a potent tool for studying the interfacial properties of antimicrobial and membrane-lytic peptides and their interactions with lipid membranes. Biochim Biophys Acta 1462:109–140

van Mau N, Vié V, Chaloin L, Lesniewska E, Heitz F, le Grimellec C (1999) Lipid-induced organization of a primary amphipathic peptide: a coupled AFM-monolayer study. J Membr Biol 167:241–249

Peggion E, Mammi S, Schievano E (1997) Conformation and interaction of bioactive peptides from insect venoms: the bombolitins. Biopolymers 43:419–431

Pethica BA (1955) The thermodynamics of monolayer penetration at constant area. Trans Faraday Soc 51:1402–1411

Pouny Y, Rapaport D, Mor A, Nicolas P, Shai Y (1992) Interaction of antimicrobial dermaseptin and its fluorescently labeled analogs with phospholipid membranes. Biochemistry 31:12416–12423

Radmacher M, Tillmann RW, Fritz M, Gaub HE (1992) From molecules to cells: imaging soft samples with the atomic force microscope. Science 257:1900–1905

Rinia HA, Kik RA, Demel RA, Snel MME, Killian JA, van der Eerden JPJM, de Kruijff B (2000) Visualization of highly ordered striated domains induced by transmembrane peptides in supported phosphatidylcholine bilayers. Biochemistry 39:5852–5858

Rinia HA, Boots JWP, Rijkers DTS, Kik RA, Snel MME, Demel RA, Killian JA, van der Eerden JPJM, de Kruijff B (2002) Domain formation in phosphatidylcholine bilayers containing transmembrane peptides: specific effects of flanking residues. Biochemistry 41:2814–2824

Scotti PD, Dearing S, Mossop DW (1983) Flock house virus: a nodavirus isolated from *Costelytra zealandica* (White). Arch Virol 75:181–189

Shai Y (1999) Mechanism of the binding, insertion and destabilization of phospholipid bilayer membranes by α-helical antimicrobial and cell non-selective membrane-lytic peptides. Biochim Biophys Acta 1462:55–70

Sitaram N, Nagaraj R (1999) Interaction of antimicrobial peptides with biological and model membranes. Structural and charge requirements for activity. Biochim Biophys Acta 1462:29–54

Sospedra P, Alsina MA, Haro I, Mestres C, Busquets MA (1999) Interaction of VP3(110–121) peptide with hepatocyte and erythrocyte membrane models. J Colloid Interface Sci 211:130–136

Trommeshauser D, Galla HJ (1998) Interaction of a basic amphipathic peptide from the carboxyterminal part of the HIV envelope protein gp41 with negatively charged lipid surfaces. Chem Phys Lipids 94:81–96

Trommeshauser D, Krol S, Bergelson LD, Galla HJ (1999) The effect of lipid composition and physical state of phospholipid monolayer on the binding and incorporation of a basic amphipathic peptide from the C-terminal region of the HIV envelope protein gp41. Chem Phys Lipids 107:83–92

Vié V, van Mau N, Chaloin L, Lesniewska E, le Grimellec C, Heitz F (2000) Detection of peptide–lipid interactions in mixed monolayers, using isotherms, atomic force microscopy, and fourier transform infrared analyses. Biophys J 78:846–856

Weakliem CL, Fuji G, Chang JE, Ben-Shaul A, Gelbart WM (1995) Effects of tension on pore formation in drug-containing vesicles. J Phys Chem 99:7694–7697

You HX, Qi X, Grabowski GA, Yu L (2002) Phospholipid membrane interactions of saposin C: in situ atomic force microscopy study. Biophys J 84:2043–2057

Zhang L, Vidu R, Waring AJ, Lejrer RI, Longo ML, Stroeve P (2002) Electrochemical and surface properties of solid-supported, mobile phospholipid bilayers on a polyion/alkylthiol layer pair used for detection of antimicrobial peptide insertion. Langmuir 18:1318–1331